Engineering and Technology Journal e-ISSN: 2456-3358

Volume 11 Issue 02 February-2026, Page No.-8958-8965

DOI: 10.47191/etj/v11i02.21, I.F. – 8.482

Explainable Lung Disease Detection on Chest X-Ray Images Using Gradient-Weighted Class Activation Mapping

Benny Sukma Negara[1], Muhammad Irsyad[2*], Wan Sofiyah[3]

[1,2,3]Informatics Engineering Study Program, Faculty of Science and Technology, Universitas Islam Negeri Sultan Syarif Kasim, Pekanbaru-Riau, Indonesia.

ABSTRACT: Early detection of respiratory diseases such as *Coronavirus Disease-19* (COVID-19) and pneumonia are crucial for accelerating treatment and preventing more serious complications. This study proposes a method for classifying chest X-ray (CXR) images using a Convolutional Neural Network (CNN) to distinguish between COVID-19, pneumonia, and lung normal. Training model involves exploring various *hyperparameter* combinations to find the optimal configuration. The best results were achieved with a *learning rate of* 0.001, 50 *epochs,* and *a batch size of* 32, with an accuracy of 96.33%. Evaluation was performed using *accuracy*, *precision*, *recall*, and *F1- score* metrics, as well as *a confusion matrix*. This study used *Gradient- Weighted Class Activation Mapping* (Grad-CAM) as a transparent interpretation tool for model decisions. The main contribution of this study is the application of Grad-CAM in *multi-class* CXR classification to improve model interpretability in lung disease diagnosis

KEYWORDS: *XAI, Covid-19, Pneumonia, Chest X-Ray, Grad-CAM*

I. INTRODUCTION

Lung health is one of the vital aspects in maintaining optimal respiratory system function, given that the lungs play a direct role in the exchange of oxygen and carbon dioxide, which are essential for life. Problems with the lungs, such as infections, inflammation, or chronic disorders, can reduce quality of life and even lead to death if not treated properly [1]. Until now, the process of identifying lung disease has generally been done manually through clinical, radiological, and laboratory examinations, which, although effective, have limitations in terms of speed, accuracy, and dependence on medical expertise [2]. in this context, technology, particularly in the fields of artificial intelligence and medical image analysis, is beginning to play an important role in supporting the early detection and diagnosis of lung diseases in a more efficient, accurate, and standardized manner.

Lung disease can be seen from changes in the structure and radiological patterns of the lung, one of which is through a CXR examination, which is a basic but crucial imaging method in evaluating lung conditions [3]. This is important in the early detection of lung disease, because changes identified at an early stage can help prevent disease progression and serious complications. There are types of lung diseases that can be identified through characteristic findings on CXR, such as pneumonia, which shows *consolidation* in the form of thick white patches that generally contain fluid, pus, and indicate a severe infection [4]. Covid-19, on the other hand, shows *Ground- Glass Opacity* (GGO), which are white spots that are not too thick, indicating inflammation, infection, and mild injury in the peripheral and lower zones of the lungs [5]. By detecting lung disease early through CXR analysis, doctors can immediately take the appropriate treatment measures, optimize treatment, and increase the chances of recovery and patient safety.

This study found that the similarity in visual features between Covid-19 and pneumonia images poses a challenge in the classification process, as both show overlapping radiological characteristics. in essence, pneumonia is an infection caused by viruses, bacteria, or fungi. Similar to Covid-19, pneumonia is life-threatening for children under 2 years of age and people over 65 years of age. Pneumonia is a contagious disease like Covid-19 with some similar symptoms. However, Covid-19 has been proven to be more fatal than pneumonia, as it can cause Acute Respiratory Distress Syndrome (ARDS) [6].

Since there is no smart diagnostic method available yet, an approach is needed that can quickly and accurately identify patients suspected of being infected with Covid-19. Although the current detection methods are quite reliable, the process still takes a relatively long time. Currently, there are three main types of methods used to detect Covid-19, namely Reverse Transcription Polymerase Chain Reaction (RT-PCR), Computed Tomography (CT) Scan, and CXR. Among the three, RT-PCR is one of the most time-consuming techniques, while CXR can detect inflammation in the lungs along with its position, shape, and size, and CT-Scan is a more effective way to diagnose Covid-19 and Pneumonia because it can provide a detailed picture of the air sacs, but this technique has a disadvantage in that it is quite expensive.

Therefore, in this study, we chose CXR as the primary medium for classification because it is more practical, faster, and economical. in addition, CXR is able to provide sufficient visual information to detect indications of infection or abnormalities in the lungs, including those caused by Covid-19 and pneumonia. with the support of deep learning technology, CXR images can be optimally utilized to assist in the automatic and accurate diagnosis process. This approach is expected to be a supporting solution in an efficient and easy-to-implement early detection system for lung diseases.

METHODOLOGY

to achieve the research objectives, a systematic methodological approach was used, which included data ollection, data *preprocessing*, modeling using model architecture, model evaluation, and XAI implementation with Grad-CAM [7].

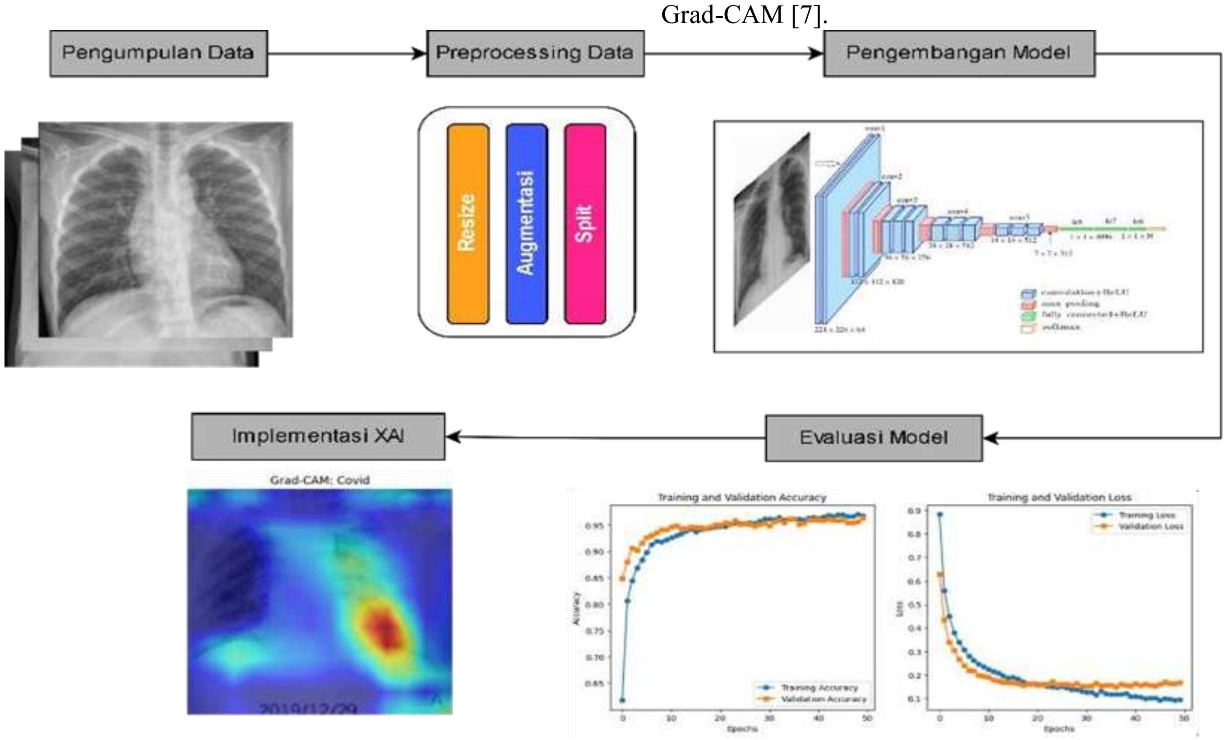

Figure 1. Research Stages

2.1 Data Collection

A dataset is needed to build an effective computational model so that it can accurately perform medical detection. The dataset used is CXR data with an original resolution of 256x256 pixels and 232x232 pixels, which is publicly available [8]. The dataset is divided into three classes: Covid-19, Normal (without lung abnormalities), and Pneumonia, with a total of 3,000 training data points, 1,000 for each class. Furthermore, we used 30 additional CXR data points that had not been trained as test data, with 10 data points per category of the same class.

2.2 Data Pre-processing

The CXR data used underwent preprocessing to standardize image size, normalize pixels, and augment data. The steps taken in preprocessing included:

a. Resize

This process is carried out by changing the size of the original image to 224×224 pixels to meet the VGG16 model input requirements. This size was chosen because it is the standard input for the architecture used, which allows spatial features to be maintained without overloading the computing process.

b. Split Data

The dataset is divided into two main parts using the train_test_split function, with a ratio of 80% for training and 20% for validation. to ensure that the class distribution remains balanced, the division is done by stratification based on the original labels. Thus, the model can be trained optimally and tested on completely new data to measure generalization

c. Data Augmentation

Data augmentation is a technique to increase the diversity and amount of data used to train *machine learning* (ML) models in order to reduce *overfitting* and improve model generalization. The augmentation technique used is random rotation up to 15° to add to the model's understanding of the data and filling empty areas using the nearest pixel value (fill_mode="nearest"). This process is applied in *real-time* during training using the ImageDataGenerator module.

2.3 Model Development

a. Convolutional Neural Net (CNN)

Convolutional Neural Networks (CNN) are an effective deep learning architecture for visual data analysis through hierarchical feature extraction and learning. CNNs consist of convolution layers, pooling, fully connected, and non-linear activation that mimic the human visual mechanism. in the convolution layer, filters are used to scan important features from images and generate feature maps as spatial representations of relevant information [9]. These filters play a role in recognizing local patterns such as edges, textures, and other important features that help in understanding complex visual structures [10].

Mathematically, the convolution process is performed by shifting the filter over the input image, then calculating the element-wise multiplication results and summing them [11]. The result of this process is a feature map that emphasizes the important characteristics of the input data, allowing the model to focus on relevant information and filter out insignificant data. with this multi-level and structured approach, CNNs are a very appropriate tool for handling challenges in medical image analysis, providing accurate and reliable results [12] Related research has discovered the potential of CNNs in developing accurate and efficient disease detection models in various applications, including medical applications using CT-scan images to predict lung cancer with the application of CNNs and achieving a fairly good average accuracy of 72.41% [13].

b. Visual Geometry Group 16 (VGG16)

Visual Geometry Group 16 (VGG16) is one of the popular CNN architectures consisting of 16 layers, specifically designed for image classification purposes. This model is widely used in medical imaging due to its ability to extract features in stages, resulting in reliable performance. Previous findings classified CT-scan images with VGG16 to detect the severity of lung cancer in three categories: benign, normal, and malignant. The results showed that the model could effectively recognize and distinguish lung conditions [14]. Another study tested various CNN architectures for lung cancer detection using *CT scans* and PET *scans*. The results showed that VGG16 excelled because it was able to accurately analyze lung cancer tissue and improve diagnostic accuracy compared to other architectures [15].

VGG16 uses small filter convolutional layers (3×3) to extract hierarchical features, ranging from simple patterns to complex structures, enabling accurate and efficient representation of medical images [16]. These filters gradually capture various features, from simple patterns such as edges to more complex structures. This enables effective representation of medical images. Each convolution operation is followed by *a* ReLU *activation function* that introduces non-linearity, enhancing the model's ability to learn and model complex relationships in the data [17].

The features obtained from the convolution layer are then processed by *a fully-connected layer* that integrates the information for classification purposes. for example, in medical image classification, VGG16 can categorize images into classes such as normal, benign, or malignant [14].

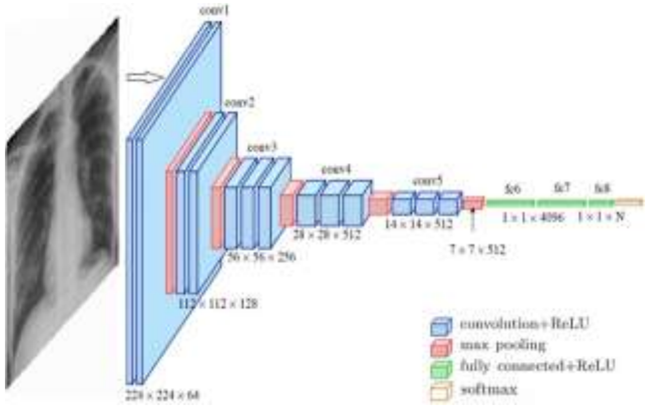

Figure 2. VGG16 architecture in CNN

Finally, the *softmax* layer converts the final results into a probability distribution, providing clear prediction probabilities for each category, thereby enabling predictions with good accuracy. This neat and systematic structure makes VGG16 useful for medical image analysis, particularly in detecting and classifying lung disorders. The combination of gradual feature extraction and strong classification capabilities ensures accurate and reliable results, which are crucial in critical medical applications [18].

c. Model Training Configuration

This study uses *transfer learning* by initializing the VGG16 model with weights that have been previously trained from the *ImageNet* dataset, utilizing *robust feature extraction* capabilities developed on a large and diverse collection of images. The model is then *fine-tuned* on the CXR dataset to specifically adapt to the process of classifying lung abnormalities. in addition, optimization using *Adaptive Moment Estimation* (ADAM) is used, which is a popular *optimizer* algorithm for CNNs, known for its adaptive momentum [19]. Recent research has explored the application of ADAM with the VGG16 architecture in various domains. in brain tumor classification, VGG16 with ADAM achieved 97.15% accuracy on the test dataset, outperforming other *optimizers* [20].

in selecting the *hyperparameter* combination, we used the *Manual Random Search* technique to obtain the configuration. A recent study compared *random search* and another technique called *Grid Search*. The *grid search* technique offers comprehensive exploration but requires significant computational resources. on the other hand, *random search* provides faster results through random selection, although it does not systematically cover all *hyperparameter* combinations [21].

Table 1. Model training hyperparameters

Hyperparameters	Value
Data ratio	80:20
Optimizer	Adam
Activation function	ReLU
Learning rate	0.00001-0.1
Epoch	25, 50, 100
Batch size	8, 32, 64

2.4 Model Evaluation

Model performance evaluation was conducted using *a classification report* that included key metrics such as *precision, recall, f1-score*, and *accuracy* for each class. in addition, *a confusion matrix* was included to provide a more detailed representation of the model's ability to classify CXR images into three categories, namely Covid-19, Normal, and Pneumonia. The calculation of these evaluation metrics is based on the standard formulas described below:

$$Accuracy = \frac{TP + TN}{TP + TN + FP + FN} \quad (1)$$

$$Precision = \frac{TP}{TP + FP} \quad (2)$$

$$Recall = \frac{TP}{TP + FN} \quad (3)$$

$$F1 - score = 2 \text{ x } \frac{Precision \text{ x } Recall}{Precision + Recall} \quad (4)$$

Explanation:
TP = Number of positive data classified correctly.
TN = Number of negative data classified correctly.
FP = Number of positive data classified incorrectly.
FN = Number of negative data classified incorrectly.

2.5 Implementation of XAI with Grad-CAM

Explainable Artificial Intelligence (XAI) is considered necessary to interpret how models make decisions transparently. XAI was developed to classify deep learning-based image interpretation methods, emphasizing the important role of explanations in model decision-making [22]. in the classification of CXR images for Covid-19, Pneumonia, and Tuberculosis, deep learning with the XAI method can achieve a test accuracy of 94.31% [23]. Grad-CAM has emerged as a powerful XAI visualization tool for interpreting CNN models [24].

Grad-CAM works by highlighting feature areas that influence the model's decision to generate a heatmap. The resulting heatmap is then superimposed on the CXR image. This approach provides a more transparent and interpretable representation of the model's decision-making process. The colors of the Grad-CAM heatmap indicate the importance or relevance of various input image elements to the model's decision. Warmer colors (e.g., red) indicate greater importance, while cooler colors (e.g., blue) indicate lesser importance. Heatmap visualization allows the identification of areas in the image that contribute most to the model's output, thereby helping to understand its decision-making process [25].

in medical diagnosis, the heatmap generated by Grad-CAM has been shown to assist radiologists in interpreting AI-based classification results [26]. Other studies have mentioned that this method outperforms other methods such as CAM and Grad-CAM++ in localizing important areas for CNN predictions [27]. This study uses Grad-CAM to improve the interpretability of model predictions, making the diagnostic process more transparent and reliable.

Generally, the steps of Grad-CAM include:

- Performing *a forward pass* to obtain the model prediction.
- Calculating the gradient of the target class score against the output of the last *convolution layer*.
- Calculating the global gradient average for each *feature map*.
- Performing a linear combination between *the feature map* and the gradient weights to produce *a class activation map*.
- Applying ReLU to *the activation map* to retain only features that support the target class.

Here is the Grad-CAM calculation formula:

$$L^c_{Grad-CAM} = ReLU\left(\sum_k \alpha \frac{c}{k} A^k\right) \quad (5)$$

- $L^c_{Grad-CAM}$ = Localization map for class c
- $\alpha \frac{c}{k}$ = Weight of feature map k
- A^k = Activation map of layer k

II. RESULTS AND DISCUSSION

This chapter presents the results of the experiments conducted and a discussion of the findings obtained. The main focus is on evaluating model performance based on varying *hyperparameter* settings. in addition, an analysis was conducted on the effect of each configuration on model accuracy to identify the combination that provides the most optimal results.

3.1 Model Training Results

This section presents a number of model training experiments. The setting scenarios use a combination of various *hyperparameters*, including *learning rate, epoch,* and *batch size*, which produce different accuracy values. The scenarios are arranged using *manual random search*, with some experiments based on existing research. The aim is to identify the best combination of parameters that can produce the most optimal model performance on the dataset used. The results of these experimental scenarios are presented in Table 2. This table shows the model performance for each *hyperparameter* combination tested, including the accuracy values obtained. Through this presentation, the patterns and effects of each parameter on the overall model performance can be analyzed.

Table 2. Model Training Experiment

No.	Ratio	*Learning Rate*	*Epoch*	*Batch Size*	*Accuracy*
1	80:20	0.01	25	8	94.83%
2	80:20	0.001	25	8	95.67%
3	80:20	0.0001	25	8	91.00%
4	80:20	0.01	50	8	95.50%
5	80:20	0.001	50	8	95.33%
6	80:20	0.01	50	32	96.00%
7	**80:20**	**0.001**	**50**	**32**	**96.33%**
8	80:20	0.0001	50	32	92.33%
9	80:20	0.00001	50	32	84.00%
10	80:20	0.0001	50	64	92.50%
11	80:20	0.001	100	8	94.67%
12	80:20	0.0001	100	32	94.17

Table 2 presents the results of model training experiments with various scenarios. All experiments used an 80:20 training and validation data ratio, ReLU activation function, and Adam optimizer. Based on the table, the combination of hyperparameters with a learning rate of 0.001, 50 epochs, and a batch size of 32 produced the highest accuracy of 96.33%. Conversely, the use of a learning rate of 0.00001 and the same combination of epoch and batch size resulted in a decrease in accuracy to only 84.00%. This indicates that a learning rate that is too low causes the training process to be ineffective.

3.2 Model Performance Evaluation

to monitor the effectiveness of the model training process, the development of accuracy and loss values in the training and validation data at each epoch was visualized. This visualization aims to identify potential underfitting or overfitting during training. The following graph shows changes in accuracy and loss values throughout 50 training epochs.

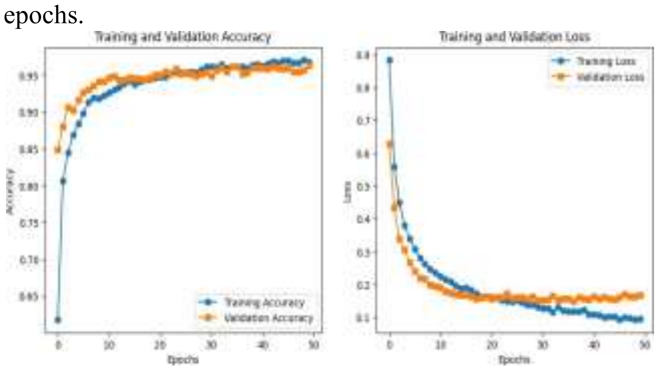

Figure 3. Accuracy and Loss Graph

It can be seen that the accuracy value in the training data increased consistently as the number of epochs increased. The accuracy in the validation data also showed a positive and relatively stable trend, indicating that the model did not experience overfitting and was able to generalize well to previously unseen data. Meanwhile, the loss graph shows a consistent decline in the curve, especially in the early stages of training, indicating that the model has successfully minimized prediction errors. from Figure 4 above, it can be concluded that the training process went well and the model can be further evaluated through classification evaluation and visual interpretation.

3.3 Classification Evaluation

The model with the best performance was then used as the basis for further evaluation, including metric analysis evaluation on accuracy, precision, recall, and F1-score.

Table 3. Mdel Classification Results

	Precision	*Recall*	*F1-Score*
Covid-19	0.99	0.98	0.99
Normal	0.95	0.99	0.97
Pneumonia	0.98	0.95	0.96
Accuracy			0.97

The evaluation results shown in Table 3 indicate that the model has good classification performance in all classes. in addition, a *confusion matrix* evaluation was also performed to further understand the model's prediction patterns. *The confusion matrix* can identify the number of correct and incorrect predictions in each class.

Table 4. Confussion Matrix

	COVID-19	Normal	Pneumonia
COVID-19	197	2	1
Normal	0	196	4
Pneumonia	2	5	193

Based on Table 4, it can be seen that the model successfully classified most of the data correctly. of the 200 Covid-19 class samples, 197 were classified correctly, while the rest were incorrectly classified as Normal and Pneumonia. A similar situation occurred in the Normal and Pneumonia classes, where the prediction error rate was also relatively low. This shows that the model has good generalization capabilities for test data and is able to effectively distinguish between classes.

3.4 Grad-CAM Visualization

This study also performed a visual interpretation of the previously tested model using the Grad- CAM method. The images produced provide a deeper understanding of the model's focus of attention on important areas of the CXR image. This helps evaluate whether the model makes decisions based on medically relevant features or not.

The following are the results of visual interpretation using Grad-CAM for each category:

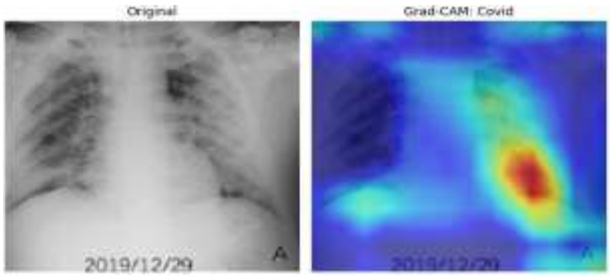

(a)

(b)

(c)

Figure 4. Grad-Cam visualization in (a) Covid-19, (b) Normal, (c) Pnemonia

Based on the above results, Grad-CAM can interpret the decisions made by the developed model by providing a visual representation of the important areas in the image that the model focuses on during classification. This visual interpretation helps in understanding the reasons behind the model's predictions and increases confidence in the model's performance in identifying the correct category.

III.CONCLUSION

This study proposes a deep learning-based Chest X-ray image classification model that shows initial capability in distinguishing between Covid-19, Normal, and Pneumonia categories based on available data. The model training process was carried out by exploring hyperparameter combinations, and the best configuration was obtained at a learning rate of 0.001, 50 epochs, and a batch size of 32. The model produced a high accuracy of 97%, with balanced precision, recall, and f1-score values for each class. Performance evaluation through a confusion matrix showed the proportion of correct and incorrect predictions for each class, while Grad-CAM visualization provided a visual interpretation of the areas that the model focused on in its decision-making. This reinforced confidence in the capabilities and transparency of the system that was built. Overall, this approach shows that CNN- based classification of CXR images can be a fast and effective diagnostic tool and has the potential to be applied in medical decision support systems. This study did not involve direct validation by medical experts. Therefore, it is recommended that future studies confirm the model's prediction results with experts such as pulmonologists or radiologists to ensure the accuracy and clinical relevance of the developed system.

REFERENCES

1. W. W. Timur, F. B. Sabiti, and N. L. Amajida, "Relationship Between Therapy Patterns and The Quality of Life of Patients with Pulmonary Tuberculosis at The Pati Community Health Center," *Jurnal Pharmacy & Science Indonesia*, Vol. 6, No. 2, Pp. 126–130, Jan. 2024, Doi: 10.52216/Jfsi.Vol6no2p126-130.
2. S. Prasad Koyyada and T. P. Singh, "An Explainable Artificial Intelligence Model for Identifying Local Indicators and Detecting Lung Disease from Chest X-Ray Images," Healthcare Analytics, Vol. 4, P. 100206, Dec. 2023, Doi: 10.1016/J.Health.2023.100206.
3. I. Benlala, F. Laurent, and G. Dournes, "Structural and Functional Changes in Copd: What We Have Learned from Imaging," Respirology, Vol. 26, No. 8, Pp. 731–741, Aug. 2021, Doi: 10.1111/Resp.14047.
4. R. Mulyadi, R. Rahmawati, E. Arief, E. Syahril, and B. Natsir, "Radiological Findings on Chest X- Rays in Hospitalized Patients Diagnosed with Community-Acquired Pneumonia," Prepotif: Journal of Public Health, Vol. 8, No. 2, Pp. 2916–2928, Jul. 2024, Doi:10.31004/Prepotif.V8i2.29570.
5. D. Cozzi Et Al., "Ground-Glass Opacity (Ggo): A Review of The Differential Diagnosis in The Era of Covid- 19," Jpn J Radiol, Vol. 39, No. 8, Pp. 721–732, Aug. 2021, Doi: 10.1007/S11604-021-01120-W.
6. M. Jafari-Oori Et Al., "Acute Respiratory Distress Syndrome and Covid-19: A Scoping Review and Meta- Analysis," 2021, Pp. 211–228. Doi: 10.1007/978-3-030-59261-5_18.
7. R. Klangbunrueang, P. Pookduang, W. Chansanam, and T. Lunrasri, "Ai-Powered Lung Cancer Detection: Assessing Vgg16 and Cnn Architectures for Ct Scan Image Classification," Informatics, Vol. 12, No. 1, P. 18, Feb. 2025, Doi: 10.3390/Informatics12010018.
8. S. Kumar Et Al., "Litecovidnet: A Lightweight Deep Neural Network Model for Detection of Covid-19 Using X-Ray Images," Int J Imaging Syst Technol, Vol. 32, No. 5, Pp. 1464–1480, Sep. 2022, Doi: 10.1002/Ima.22770.

9. N. Nurkhasanah and M. Murinto, "Classification of Facial Skin Diseases Using The Convolutional Neural Network Method," Sainteks, Vol. 18, No. 2, P. 183, Feb. 2022, Doi: 10.30595/Sainteks.V18i2.13188.
10. K. J. Aditya, I. Kanedi, and A. Sudarsono, "Edge Detection Segmentation in Digital Images of Adult Bone Fractures Using The Sobel Method and The Prewitt Method," Djtechno: Journal of Information Technology, Vol. 3, No. 2, Pp. 224–233, Dec. 2022, Doi: 10.46576/Djtechno.V3i2.2735.
11. L. Stanković and D. Mandic, "Convolutional Neural Networks Demystified: A Matched Filtering Perspective-Based Tutorial," Ieee Transactions on Systems, Man, and Cybernetics: Systems, Vol. 53, No. 6, Pp. 3614–3628, June 2023, Doi: 10.1109/Tsmc.2022.3228597.
12. G. Kourounis, A. A. Elmahmudi, B. Thomson, J. Hunter, H. Ugail, and C. Wilson, "Computer Image Analysis with Artificial Intelligence: A Practical Introduction to Convolutional Neural Networks for Medical Professionals," Postgrad Med J, Vol. 99, No. 1178, Pp. 1287–1294, Nov. 2023, Doi: 10.1093/Postmj/Qgad095.
13. A. Bherje Et Al., "Design of Deep Learning-Based Approach to Predict Lung Cancer on Ct Scan Images," in 2024 5th International Conference on Innovative Trends in Information Technology (Icitiit), Ieee, Mar. 2024, Pp. 1–5. Doi: 10.1109/Icitiit61487.2024.10580370.
14. H. Huang, M. Wang, Q. Ye, and Z. Zhou, "Diagnosis of Lung Cancer Based on Ct Scans Using Convolutional Neural Networks," in 2022 International Conference on Data Analytics, Computing and Artificial Intelligence (Icdacai), Ieee, Aug. 2022, Pp. 338–341. Doi: 10.1109/Icdacai57211.2022.00073.
15. C. Tejaswini, P. Nagabushanam, P. Rajasegaran, P. R. Johnson, and S. Radha, "Cnn Architecture for Lung Cancer Detection," in 2022 Ieee 11th International Conference on Communication Systems and Network Technologies (Csnt), Ieee, Apr. 2022, Pp. 346–350. Doi: 10.1109/Csnt54456.2022.9787650.
16. S. A. E. Albakia and R. A. Saputra, "Identification of Medicinal Plant Leaf Types Using The Convolutional Neural Network (Cnn) Method with The Vgg16 Model," Jurnal Informatika Polinema, Vol. 9, No. 4, Pp. 451–460, Aug. 2023, Doi: 10.33795/Jip.V9i4.1420.
17. D. R. Sarvamangala and R. V. Kulkarni, "Convolutional Neural Networks in Medical Image Understanding: A Survey," Evol Intell, Vol. 15, No. 1, Pp. 1–22, Mar. 2022, Doi: 10.1007/S12065-020-00540-3.
18. S. Tammina, "Transfer Learning Using Vgg-16 with Deep Convolutional Neural Network for Classifying Images," International Journal of Scientific and Research Publications (Ijsrp), Vol. 9, No. 10, P. P9420, Oct. 2019, Doi: 10.29322/Ijsrp.9.10.2019.P9420.
19. S. Chaudhury and T. Yamasaki, "Robustness of Adaptive Neural Network Optimization Under Training Noise," Ieee Access, Vol. 9, Pp. 37039–37053, 2021, Doi: 10.1109/Access.2021.3062990.
20. M. Sah and C. Direkoglu, "A Survey of Deep Learning Methods for Multiple Sclerosis Identification Using Brain Mri Images," Neural Comput Appl, Vol. 34, No. 10, Pp. 7349–7373, May 2022, Doi: 10.1007/S00521- 022-07099-3.
21. N. Subaşı, "Comprehensive Analysis of Grid and Randomized Search on Dataset Performance," European Journal of Engineering and Applied Sciences, Vol. 7, No. 2, Pp. 77–83, Dec. 2024, Doi: 10.55581/Ejeas.1581494.
22. B. H. M. Van Der Velden, H. J. Kuijf, K. G. A. Gilhuijs, and M. A. Viergever, "Explainable Artificial Intelligence (Xai) in Deep Learning-Based Medical Image Analysis," Med Image Anal, Vol. 79, P. 102470, Jul. 2022, Doi: 10.1016/J.Media.2022.102470.
23. M. Bhandari, T. B. Shahi, B. Siku, and A. Neupane, "Explanatory Classification of Cxr Images Into Covid-19, Pneumonia and Tuberculosis Using Deep Learning and Xai," Comput Biol Med, Vol. 150, P. 106156, Nov. 2022, Doi: 10.1016/J.Compbiomed.2022.106156.
24. Y. Shen and X. Huang, "A Comparative Visualization Analysis of Neural Network Models Using Grad- Cam," Science and Technology of Engineering, Chemistry and Environmental Protection, Vol. 1, No. 10, Dec. 2024, Doi: 10.61173/Yzp9wt79.
25. Md. Z. Hasan Et Al., "Fast and Efficient Lung Abnormality Identification with Explainable Ai: A Comprehensive Framework for Chest Ct Scan and X-Ray Images," Ieee Access, Vol. 12, Pp. 31117–31135, 2024, Doi: 10.1109/Access.2024.3369900.
26. J.-C. Chien, J.-D. Lee, C.-S. Hu, and C.-T. Wu, "The Usefulness of Gradient-Weighted Cam in Assisting Medical Diagnoses," Applied Sciences, Vol. 12, No. 15, P. 7748, Aug. 2022, Doi: 10.3390/App12157748.
27. Y. Zhang, D. Hong, D. Mcclement, O. Oladosu, G. Pridham, and G. Slaney, "Grad-Cam Helps Interpret The Deep Learning Models Trained to Classify Multiple Sclerosis Types Using Clinical Brain

Magnetic Resonance Imaging," J Neurosci Methods,
Vol. 353, P. 109098, Apr. 2021,
Doi: 10.1016/J.Jneumeth.2021.109098.